International Journal of Nanomedicine

Dovepress
open access to scientific and medical research

Open Access Full Text Article

ORIGINAL RESEARCH

# Antioxidant Nanoparticles Restore Cisplatin-Induced Male Fertility Defects by Promoting MDC1-53bp1-Associated Non-Homologous DNA Repair Mechanism and Sperm Intracellular Calcium Influx

Yu-Syuan Wei[1], Yu-Liang Chen[2], Wei-Yun Li[1], Ya-Yi Yang[3], Sung-Jan Lin[4–6], Ching-Ho Wu[7], Jiue-In Yang[8], Tse-En Wang[1], Jiashing Yu[2], Pei-Shiue Tsai[1,3,4]

[1]Graduate Institute of Veterinary Medicine, National Taiwan University, Taipei, 10617, Taiwan; [2]Department of Chemical Engineering, College of Engineering, National Taiwan University, Taipei, 106, Taiwan; [3]Department of Veterinary Medicine, National Taiwan University, Taipei, 10617, Taiwan; [4]Research Center for Developmental Biology and Regenerative Medicine, National Taiwan University, Taipei, 10617, Taiwan; [5]Department of Biomedical Engineering, College of Medicine and College of Engineering, National Taiwan University, Taipei, 10051, Taiwan; [6]Department of Dermatology, National Taiwan University Hospital and College of Medicine, Taipei, 10002, Taiwan; [7]Graduate Institute of Veterinary Clinical Science, School of Veterinary Medicine, National Taiwan University, Taipei, 10617, Taiwan; [8]Department of Plant Pathology and Microbiology, National Taiwan University, Taipei, 10617, Taiwan

Correspondence: Jiashing Yu, Department of Chemical Engineering, College of Engineering, National Taiwan University, No. 1, Sec. 4, Roosevelt Road, Daan District, Taipei, 10617, Taiwan, Tel +886 2 33669477, Email jiayu@ntu.edu.tw; Pei-Shiue Tsai, Department and Graduate Institute of Veterinary Medicine, School of Veterinary Medicine, National Taiwan University, No. 1, Sec. 4, Roosevelt Road, Daan District, Taipei, 10617, Taiwan, Tel +886 2 33661290, Fax +886 2 23661475, Email psjasontsai@ntu.edu.tw



**Introduction:** Cisplatin, a commonly used anticancer compound, exhibits severe off-target organ toxicity. Due to its wide application in cancer treatment, the reduction of its damage to normal tissue is an imminent clinical need. Cisplatin-induced testicular oxidative stress and damage lead to male sub- or infertility. Despite earlier studies showing that the natural polyphenol extracts honokiol serve as the free radical scavenger that reduces the accumulation of intracellular free radicals, whether honokiol exhibits direct effects on the testis and sperm is unclear. Thus, the aim of the current study is to investigate the direct effects of honokiol on testicular recovery and sperm physiology.

**Methods:** We encapsulated this polyphenol antioxidation compound into liposome-based nanoparticles (nHNK) and gave intraperitoneally to mice at a dosage of 5 mg/kg body mass every other day for consecutive 6 weeks.

**Results:** We showed that nHNK promotes MDC1-53bp1-associated non-homologous DNA double-strand break repair signaling pathway that minimizes cisplatin-induced DNA damage. This positive effect restores spermatogenesis and allows the restructuring of the multi-spermatogenic layers in the testis. By reducing mitochondrial oxidative damage, nHNK also protects sperm mitochondrial structure and maintains both testicular and sperm ATP production. By a yet-to-identify mechanism, nHNK restores sperm calcium influx at the sperm midpiece and tail, which is essential for sperm hypermotility and their interaction with the oocyte.

**Discussion:** Taken together, the nanoparticulated antioxidant counteracts cisplatin-induced male fertility defects and benefits patients undertaking cisplatin-based chemotherapy. These data may allow the reintroduction of cisplatin for systemic applications in patients at clinics with reduced testicular toxicity.

**Keywords:** nanomedicine, antioxidant, cisplatin, reproduction, DNA repair, polyphenol

## Introduction

Steadily spermatogenesis relies on functional testis; however, successful fertility requires motile sperm with the ability to bind to the zona pellucida (ZP) of the oocyte.[1,2] Both processes involve the temporal and spatial coordination between various proteins and ion channels on the sperm membrane surface to drive calcium influx at specific sperm regions.[3–5]

Received: 1 March 2023
Accepted: 19 July 2023
Published: 7 August 2023

For sperm motility, calcium channels, such as the cation channel of sperm (CatSper), allow calcium influx into the sperm tail and drive the subsequent flagellar movement toward a powerful whip-like motion.[4–6] Moreover, the interaction between store-operated channel proteins (Orai) and their activator [STIM (stromal interaction molecule)] would amplify intracellular calcium ([$Ca2^{+}$]i) transients at the sperm neck/mid-piece without affecting flagellar [$Ca2^{+}$]i response,[7] both studies support that fact that calcium dynamics at both sperm midpiece and tail are crucial for sperm motility and regular sperm physiology upon fertilization processes. Apart from acquiring hyper-motility, calcium influx at the sperm head ensures sperm-zona binding, acrosome reaction, and the release of hydrolytic enzymes required for sperm penetration through the ZP of the oocyte.[8,9] Besides the critical role of calcium for sperm motility, healthy mitochondria located at the sperm midpiece is also essential for maintaining normal sperm function. Sperm carries approximately 50–75 mitochondria. These mitochondria are responsible for producing ATPs needed for sperm motility and defending the free radical-enriched microenvironment in both male and female reproductive tracts to maintain the redox balance and prevent oxidative stress (OS) of the sperm cells.[10–12]

Cisplatin or cis-diamminedichloroplatinum(II) is an effective platinum-containing anti-cancer compound; by intercalating into unwind DNA and stopping the cell cycle, cisplatin can target fast-dividing cancer cells and leads to cell apoptosis. However, this cellular process is non-specific and thus also interferes with normal cells causing multiple organ toxicities, including the kidney and the testis.[13–15] Our earlier publication showed that cisplatin administration led to oxidative stress of Sertoli cells, Leydig cells, and germ cells of different maturation stages.[15] Moreover, cisplatin administration increased mitochondrial damage and endoplasmic reticulum (ER) stress, promoted cellular apoptosis, and resulted in testicular fibrosis.[15,16] Under the healthy condition, individuals possess defense mechanisms that facilitate the quenching of intracellular reactive oxygen species (ROS) and maintain equilibrium between pro- and antioxidants; however, excessive production of ROS that exceeds normal antioxidant capability results in OS and the activation of intrinsic apoptosis cascade.[16–18] Oxidative stress has been correlated to male in/sub-fertility, characterized by impaired sperm motility, low sperm count, and increased abnormal sperm morphology.[19–22] Therefore, maintaining redox balance and anti-oxidation microenvironment in the male reproductive system is an imminent clinical need to preserve the fertility of patients undertaking cisplatin-based chemotherapy treatments.

Cells maintain intracellular-free radical balance by both enzymatic and non-enzymatic anti-oxidation systems. Glutathione peroxidase (GPx), superoxide dismutase (SOD), and catalase are crucial anti-oxidation enzymes known to regulate testicular and epididymal redox activity and to maintain the proper amount of ROS needed for sperm physiology.[23–27] Other non-enzymatic antioxidants, such as vitamins E, C, flavonoids, and polyphenols, can also serve as ROS scavengers to protect testis and sperm cells from chemotherapy-induced damages.[14,28–31] Our earlier publications demonstrated that a natural polyphenol compound, honokiol (HNK), could effectively attenuate both renal and testicular damage induced by cisplatin.[14,15,30] However, besides reducing the amount of intracellular-free radicals, the direct effects of HNK on reproduction or sperm physiology are yet to be elucidated. Therefore, in this study, we aim to investigate whether nanosome-encapsulated HNK exhibits direct biological effects on testis and sperm physiology that are essential for male fertility.

# Materials and Methods

## Chemicals, Reagents, Antibodies

All chemicals and reagents were acquired from Sigma unless otherwise stated. Cisplatin (Cat. #479306, purity ≥99.9%) was obtained from Sigma Aldrich (St Louis, MO, USA), 2-(4-hydroxy-3-prop-2-enyl-phenyl)-4-prop-2-enyl-phenol (Honokiol, Cat. #SLK S2310, purity: 99.81%) was purchased from Selleckchem (Houston, TX, USA). Rabbit polyclonal anti-kinesin family member 11 (KIF11) antibody (#HPA10568) and anti-elongation factor 2 (EEF2) antibody (#ab33523) were acquired from Sigma Aldrich and Abcam (Boston, MA, USA), respectively. Mouse monoclonal anti-53bp1 antibody (#NBP2-25028) and anti-BRAC1 antibody (#NB100-404) were obtained from Novus Biologicals, LLC (Centennial, CO, USA). Calcium influx measurement on live sperm cells was performed using a commercially available Fluo-4 Calcium Imaging Kit (# F10489, Molecular Probe™, Thermo Fisher Scientific, Waltham, MA, USA). All secondary antibodies were purchased from Jackson ImmunoResearch Laboratories Inc. (West Grove, PA, USA).

## Establishment and Validation of the Cisplatin-Induced Testicular Injury

Cisplatin-induced testicular injury and subfertility mouse models were established and validated as earlier described.[15] In short, 12-week-old male institute of cancer research, Caesarean Derived-1 (ICR, CD1) mice were purchased from BioLASCO Co., Ltd. (Taipei, Taiwan) and were housed in groups (3 mice/cage) throughout the experiments. Mice were accommodated at a constant temperature (22–24°C) with a 12 h-12 h light–dark cycle and were given water and standard mice lab chow (Oriental yeast, Tokyo, JP) ad libitum. All animal experiments were performed under the permission of institutional animal care and use committee (IACUC) protocols (NTU109-EL-00158) at National Taiwan University. A 6-week testicular injury mouse model had been described in our earlier publications[14,15] and was summarized in Supplementary Figure 1A. Preparation and characterizations of the nano-sized encapsulated honokiol particle were described in detail in our earlier publication.[32] Sixty mice were randomly allocated into four groups (n=15 in each group); control or compound administration was illustrated accordingly (Supplementary Figure 1A). Physical and histological validations on the success of the mouse model were performed and described in our earlier publications.[14,15] Body mass was measured and recorded weekly throughout the experiment (Supplementary Figure 1B).

## Immuno-Blotting

An equivalent amount (μg) of protein extract was resuspended with lithium dodecyl sulfate (LDS) loading buffer (NuPAGE™, Thermo Fisher Scientific) in the presence of 50 mM dithiothreitol (DTT) reducing agent. Samples were heated in a 95°C- dry bath for 10 min and cooled on ice until use. Bio-Rad Mini-PROTEIN® electrophoresis system was applied (Bio-Rad Laboratories Ltd., Hertfordshire, DX). Proteins were separated by 10% sodium dodecyl sulfate-polyacrylamide gel and wet-blotted onto a polyvinylidene difluoride (PVDF) membrane (Immobilon-P, Millipore, Burlington, MA, USA). After blocking for 1 h with blocking buffer (5 mM Tris, 250 mM sucrose, pH 7.4 with 0.05% v/v Tween-20 [TBST], supplemented with 5% milk powder) at RT, blots were incubated with different antibodies as follows: anti-53bp1 (1:500), anti-BRAC1 (1:500), anti-EEF2 (1:10,000) at 4°C for overnight. After rinsing with TBST, secondary antibodies (anti-mouse horseradish peroxidase 1:10,000 or anti-rabbit horseradish peroxidase 1:10,000) were added, and blots were incubated at RT for another 1h. After rinsing with TBST, protein signals were visualized by chemiluminescence (Merck, Ltd., Kenilworth, NJ, USA) and detected under the ChemiDoc™ XRS+ system (Bio-Rad Laboratories, Hercules, CA, USA). The relative intensity of the signal was determined using ImageJ software. When necessary, blots were stripped (Thermo Fisher Scientific) and re-probed for other proteins of interest.

## Sperm Acquisition and Motility-Related Parameter Analyses

To evaluate cisplatin and honokiol effects on sperm motility-related parameters, a portable iSperm® device (Aidmics Biotechnology Co., Ltd., Taipei, Taiwan) was used. After mice were euthanized with carbon dioxide ($CO_2$), epididymal sperm cells were obtained on a temperature-controlled (37 °C) dissecting microscopy platform as described earlier.[33] Default parameter settings were followed iSperm instruction manual for mouse species. For iSperm® analysis of sperm cells, four individual frames were analyzed per measurement. Based on manufacturer's instructions, $35\times10^6$ sperm cells/mL is the optimal sperm concentration for accurate and reliable measurement; therefore, depending on the original sperm concentration, a 5–10 times diluted semen sample of 7.5 μL was spotted on the surface of the base chip, and a cover chip was pressed on top as per the instruction manual. The combined chipset was screwed into the microscope attached to the iPad Mini camera (Apple Inc., Cupertino, CA, USA) for analysis. The semen samples of different experimental groups were assessed in triplicate; the sample chip was analyzed in the iSperm application four times consecutively to allow for later calculation of the coefficient of variation (CV). The parameters, including total motility (%), progressive motility (%, cut-offs when average path velocity (VAP) >50 μm/sec and STR > 50%), and concentration (million/mL) were measured. Detail sperm swimming patterns, such as velocity average path (VAP, μm/s), velocity straight line (VSL, μm/s), velocity curvilinear (VCL, μm/s), and the amplitude of lateral head displacement (ALH, μm) were also analyzed. For each group, sperm cells from four individual animals were measured.

## RNAseq Analysis

To analyze the affected genes, freshly obtained testicular homogenates from three independent individuals were applied to poly-T oligo-attached magnetic beads (TruSeq® Stranded mRNA Library Prep Kit [Illumina, San Diego, CA, US]) to obtain 2 μg of purified RNA as input materials. Fragmentation of purified RNA was carried out using divalent cations and was copied into first-strand cDNA by reverse transcriptase and random primers. The cDNA synthesis was performed by DNA Polymerase I and RNase H, and the cDNA library was established as previously described.[34] NextSeq500 (Illumina Inc., CIC bioGUNE, Bilbao, Spain) was used to obtain 10 million reads for each sample. High-quality reads were aligned to the *Mus musculus* genome GCRm38 assembly from the ICR strain using the Ensembl platform. The mapping coverage of the reads was >90% in all cases. Differential expression genes (DEG) were obtained by the parametric threshold of absolute $\log_2$ fold change ≥2 between experimental comparisons (in this study, vehicle control vs cisplatin injury; cisplatin injury vs nHNK treatment [Cis/nHNK]). To identify network interactions, the pool of DEG genes was loaded to QIAGEN's Ingenuity Pathway Analysis (www.qiagen.com/ingenuity).

## Tissue Preparation and Indirect Immunofluorescent Staining

Five μm paraffin-embedded tissue sections were deparaffinized, rehydrated, and underwent antigen retrieval procedures as earlier described.[14] After minimizing non-specific background signaling using 1% BSA as a blocking reagent for 60 min at RT, tissue sections were permeabilized with 100% ice-cold methanol at −20°C for 10 min. Anti-KIF11 (1:50) antibody were used for overnight incubation at 4°C. Sections were subsequently incubated with donkey-anti-mouse /rabbit Alexa-488 (1:150 diluted with TBST, five mM Tris, 250 mM sucrose, pH 7.4 with 0.05% v/v Tween-20) for 1.5 hr at RT at dark. Nuclei were counterstained with an aqueous fluoroshield mounting medium in the presence of diamidino-2-phenylindole (DAPI) (#Ab104139, Abcam, Cambridge, UK). All samples were evaluated under Olympus IX83 epifluorescent microscopy. Background subtraction and contrast/brightness enhancement (up to ~20% enhancement) were performed identically for all images in the same experiment.

## Quantitative Calcium Influx Measurement

Sperm motility requires an influx of extracellular calcium through specific calcium channels at both the sperm midpiece and tail. To measure dynamic calcium influx in live sperm, $Ca^{2+}$ indicator Fluo-4 AM (Thermo Fisher Scientific) was used. Epididymal sperm cells from 4 experimental groups were obtained, as above-mentioned. To standardize and validate the measurement and to correct potential background signals from the medium or autofluorescent from sperm per se, based-line measurements of fluorescent signal, including Hepes-based tyrodes medium (TYH, 119 mM NaCl, 4.8 mM KCl, 1.2 mM $MgSO_4$, 20 mM HEPES with/without 25 mM $NaHCO_3$, 3 mg/mL bovine serum albumin for control and capacitation medium, respectively, pH 7.4, 300 mosmol/kg) and Fluo-4 AM stained and unstained sperm suspension were performed (Supplementary Figure 2). To measure the dynamic calcium influx in live sperm, $1\times10^9$ sperm cells were used for each measurement. Ten μM calcium indicator Fluo-4 AM was co-incubated with sperm cells for 60 minutes at a 37.5°C humidified incubator. Stained sperm cells were spun down (700 g, 5 minutes), and unbound dyes were removed. Sperm cells were resuspended with indicator and BSA-free pre-warmed TYH medium for a further 30 minutes, as suggested by the company, to reduce the non-specific binding and allow complete de-esterification of intracellular AM esters. A final 100 μL sperm suspension was added into each well of a black 96-well ELISA plate. Kinetic measurement of the changes of fluorescent intensity (excitation wavelength at 485 nm, emission wavelength at 538 nm, cut off at 530 nm) was measured and recorded at dark using a temperature-controlled (37 °C) SpextraMax M5 microplate reader (Molecular Devices, San Jose, CA, USA) with a 2 minutes recording interval for consecutive 150 minutes. For each experimental group, sperm cells from at least 5–6 individual animals were measured.

## ATP Level Assay

To access the level of sperm intracellular ATP, a commercially available colorimetric ATP assay kit (Ab63355, Abcam) was used. To standardize the measurement, $1x10^8$ epididymal sperm cells were obtained from animals of 4 experimental groups, and the standard protocol was followed according to manufacturer's instructions. In short, epididymal sperm cells

were washed in ice-cold PBS before being lysed in ATP assay buffer. Non-lysed sperm fragments were spun down at 13,000 g at 4°C. The supernatant was collected and used for ATP assay. ATP reaction mixture, including background control mixtures (without ATP converter), was prepared as instructed. After 30 min incubation at room temperature (RT) at dark, sample optical density (O.D.) was measured within 2 hr after incubation at 570 nm. A standard curve was created using provided ATP standard with reading O.D. ATP concentration in each sample was thereafter calculated and expressed as nmol/mL. For each experimental group, sperm cells from 5 individual animals were measured.

### Transmission Electron Microscopy

A transmission electron micrograph (TEM) was used to examine sperm structural changes, especially on the sperm midpiece and sperm tail. Epididymal sperm from control and cisplatin-injured animals were obtained by dissecting epididymis on a temperature-controlled stage (37 °C). Sperm cells were allowed to swim out for 10 minutes in pre-warmed PBS before centrifugation at 1000 g for 10 minutes. Sperm pellets were fixed overnight at 4°C in Karnovsky fixative (contains 2% (v/v) paraformaldehyde and 2.5% (v/v) glutaraldehyde diluted in cacodylate buffer). Fixed pellets were washed with 0.1 M Na-cacodylate (pH 7.4) and post-fixed with 1% osmium tetraoxide in 0.1 M Na-cacodylate (pH 7.4) for 1 h. After washing with milli-Q $H_2O$, pellets were incubated with 2% (w/v) uranyl acetate for an additional 1 hr. Sample dehydration was carried out with acetone (50–100%) and subsequently embedded in Durcupan ACM resin (Fluka, Bachs, Switzerland). Ultrathin sections of 70–80 nm were obtained on an Ultramicrotome (Leica EM UC7, Wetzler, Germany) and studied using TEM (JEM-1200EX II, Jeol USA, Peabody, MA, USA) for final visualization.

### Statistical Analysis

Data were expressed as mean ± SD. One-way analysis of variance (ANOVA) followed by nonparametric analysis with Kruskal–Wallis multiple comparisons test was used to evaluate statistical differences via GraphPad Prism (GraphPad Software, San Diego, CA, USA). Differences were considered statistically significant at a p-value $<0.05$.

## Results

### Antioxidant Nanoparticles Restored 2525 Fertility-Relevant Genes in the Cisplatin-Injured Testis

The DEG analysis and volcano plots showed a high degree of similarity in gene profiles between control (grey) and nHNK alone (blue) groups. An apparent difference in testicular gene profile was observed after cisplatin injury (red); interestingly, in the nHNK treatment group, the testicular gene profile was restored and was similar to control and nHNK groups with minor differences (Figure 1A and B). Based on DEG analysis, 3979 testicular genes were down-regulated, and 4195 were up-regulated upon cisplatin injury. On the other hand, 3157 testicular genes were down-regulated, and 2672 were up-regulated upon nHNK treatment (Figure 1C). The Kyoto encyclopedia of genes and genomes (KEGG) pathway analysis showed that cellular and molecular pathways related to the regulation of membrane microdomain, wound healing response, cellular organ homeostasis, extracellular matrix, oxidative stress, reproductive structure development, epithelial cells proliferation, actin cytoskeleton, and cell–cell junction were among the most affected signaling pathways (Supplementary Table 1). As we are interested in genes that were down-regulated by cisplatin injury but were rescued upon nHNK treatment, an overlapped 2525 genes were identified (Figure 1C and D). Among all identified genes, sperm mitochondrially encoded genes, such as cytochrome c oxidase I, NADH dehydrogenase, spermatogenesis-related genes, such as calmegin, kinesin family member 11, sperm calcium-binding protein, sperm-specific cation channels, such as CatSper, and sperm structural genes that were relevant to sperm movement or motility were significantly affected (Figure 1E, Supplementary Table 2, Supplementary Figure 3A).

Furthermore, DEGs were assigned to 67 gene ontology (GO) terms, including 23 biological processes (BP), 14 cellular components (CC), and 30 molecular functions (MF) with ≥3 corresponding gene numbers were screened. The top 10 enriched GO terms for BP, CC, and MF are illustrated in Supplementary Figure 3B. Based on GO terms, sperm motility-related biological processes or cellular components were most dominant, and ATPase and calcium channel activities were pronouncedly rescued after honokiol treatment (Supplementary Figure 3B).

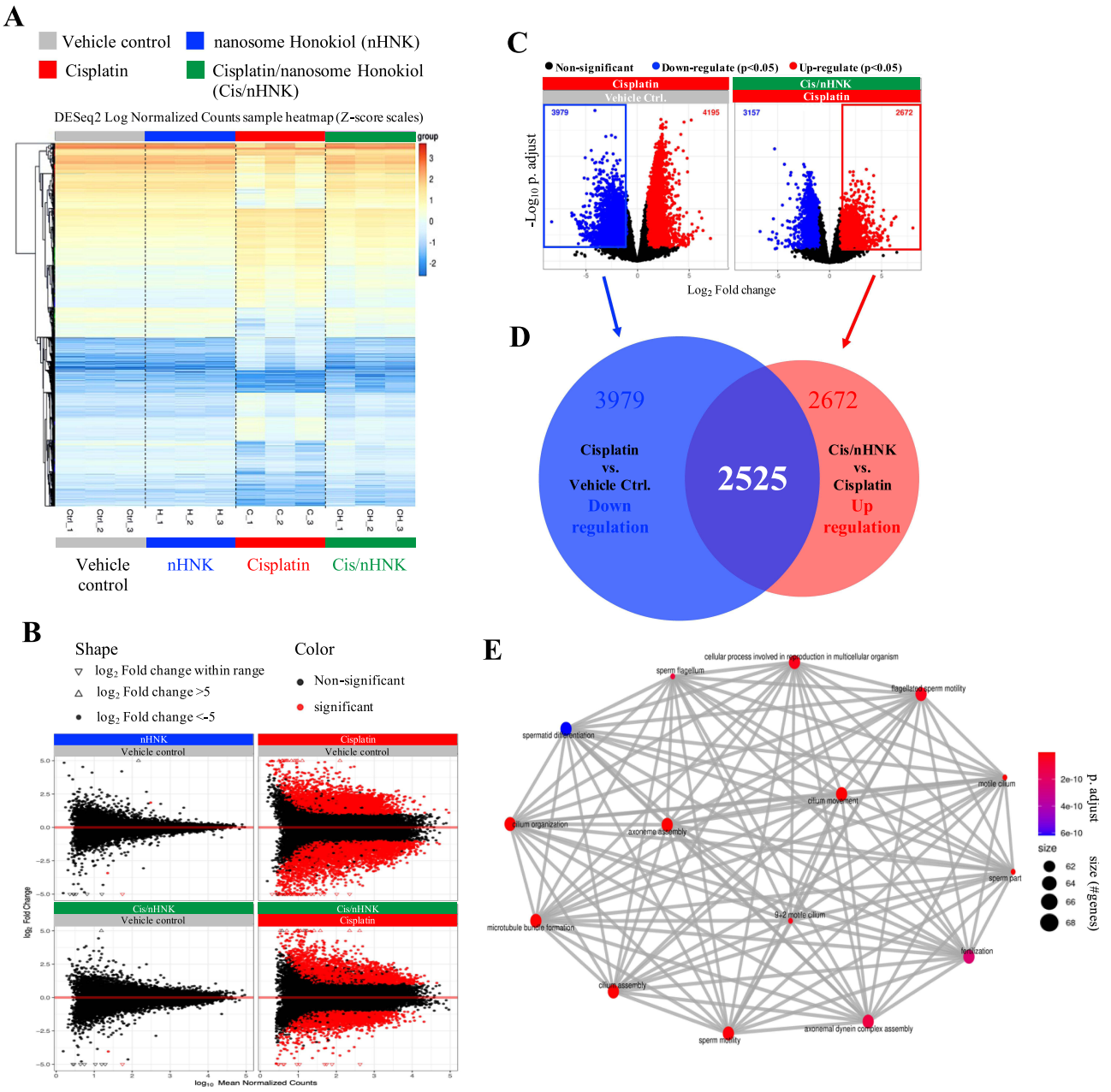


**Figure 1** Next-generation sequence analyses revealed similarities and differences in gene profiles between experimental groups and revealed the potential function of affected genes. (**A**) Differential expression gene (DEG) profiles of control, nHNK, cisplatin, and Cis/nHNK groups demonstrated high similarity in gene profiles between control, nHNK, and Cis/nHNK groups and a distinct pattern after cisplatin injury. (**B**) Volcano plots confirmed different testicular gene expression patterns between control, cisplatin-injured, and Cis/nHNK groups. (**C** and **D**) DEG analysis showed 14,003 affected genes; 2525 were down-regulated upon cisplatin-injury and up-regulated after nHNK administration. (**E**) Among 2525 genes of interest, many were relevant for spermatid differentiation, fertilization, and the maintenance of sperm structure. Testes of three animals from each experimental group were used for next-generation sequence analyses.

## Nanoparticulated Antioxidants Recused Testicular Cell Proliferation and Spermatogenesis

We observed an apparent restoration of testicular spermatogenesis layers in the testis of the nHNK treatment group; therefore, we examined whether the increased spermatogenic layers were due to an increase or restoration of cell proliferation of the testis. As shown in Figure 2A, B, when compared with the control testis (37.7%), there was a significant decrease in Ki67-positive cells in the cisplatin-injured testis (3.8%); however, the number of Ki67-positive cells were recovered after nHNK treatment (32.5%) suggesting a restoration of testicular cell proliferation

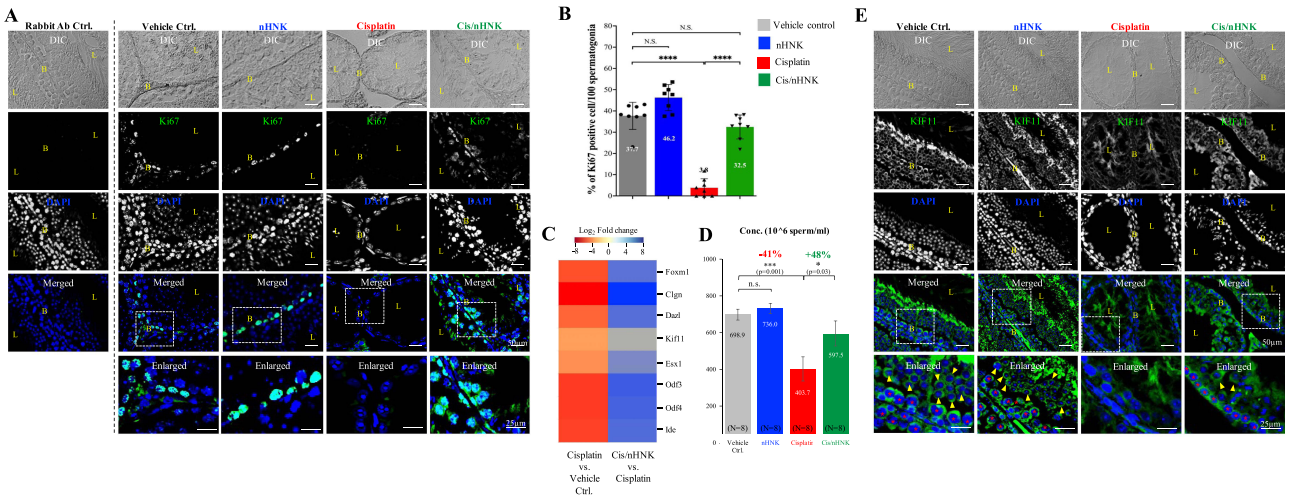


**Figure 2** Spermatogenesis was affected by cisplatin but can be rescued upon nHNK treatment. (**A**) Ki67, a cell proliferation marker, was used to evaluate testicular cell proliferation ability. Compared with the control testis, weak to no Ki67 signal can be detected in cisplatin testis; however, after nHNK treatment, the restoration of Ki67-positive cells was observed (**B**). Quantitative analysis showed a significant decline in Ki67-positive cells in the cisplatin group (37.7%, 46.2%, and 3.8% in control, nHNK alone, and cisplatin group, respectively), respectively a significant recovery in the percentage of Ki67-positive cells was measured after nHNK treatment (32.5%). (**C**) Genes previously known to be responsible for spermatogenesis, such as Clgn, Dazl, Kif11, and Ide, were down-regulated in cisplatin-injured testis and up-regulated after nHNK treatment. (**D**) Compared with the control and nHNK group which ~700-740x$10^6$ sperm/mL can be measured, cisplatin testis produced significantly lower number of sperm cells (403x$10^6$ sperm/mL, 41% decline). nHNK treatment partially restored sperm production (597x$10^6$ sperm/mL, 48% increase). (**E**) Besides disruption of regular spermatogenic layers, kinesin family member 11, one of the marker proteins for spermatogonia and the process for spermatogenesis, was diminished from spermatogonia (marked in red asterisks) and spermatogenic cells (marked in yellow arrowheads) after cisplatin injection. Re-appearance of the KIF11 signals on both spermatogonia and spermatogenic cells can be detected after nHNK treatment. (**B**) indicated the basal layer of the seminiferous tubules, and L indicated the positive of the lumen. Representative images were presented, and 16 images were evaluated in each group. Bars represent standard deviation (S.D.), and results were presented as mean ± standard deviation (S.D.). *p<0.05, ***p<0.001, ****p<0.0001.
**Abbreviation**: N.S., not statistically different.

(Figure 2A and B). From the results of RNAseq, we identified several spermatogenesis-responsible genes, such as Clgn, Dazl, KIF11, and Ide, which were down-regulated upon cisplatin injury but were up-regulated again after nHNK was administrated as the treatment (Figure 2C). The changes in spermatogenesis-responsible genes were reflected in sperm concentration measured. Both control and nHNK alone mice could produce a sperm concentration of ~700-740x$10^6$ sperm cells/mL. However, after cisplatin injury, sperm production declined to 400x$10^6$ sperm cells/mL (41% decrease compared to control). A significant increase in sperm production was measured upon nHNK treatment (~600×$10^6$ sperm cells/mL, +48% when compared with cisplatin injured group, Figure 2D). We showed nHNK promoted cell proliferation (Figure 2A) to confirm Ki67 positive signals correlate with increased spermatogenesis, the presence of spermatogenesis marker, the kinesin family member 11 (KIF11) was checked.[35] We observed that KIF11 was pronouncedly present in the spermatogonia (red asterisks) and later stages of spermatocytes (yellow arrowheads) in the control mouse testis; however, after cisplatin injury, KIF11 disappeared from the spermatogonia, and only a weak signal was detected in the seminiferous tubule lumen; in contrast, KIF11 signal can be seen again in nHNK-treated testis indicated nHNK restored the spermatogenesis function of the testis (Figure 2E). The reappearance of KIF11 signals and the restoration of normal spermatogenesis not only reflected in the structural restoration of seminiferous tubules (Figure 2E, DIC panel) but also in the rebound phenotype in sperm concentrations in Cis/nHNK group (Figure 2D, green bar).

## Honokiol Promoted MDC1-53bp1-Associated Non-Homologous DNA Repair

Cisplatin leads to DNA breaks and arrests the cell cycle, disrupting regular spermatogenesis. Restoration of regular spermatogenesis caused by cisplatin may require activation of the DNA repair mechanism. The mechanism of double-strand DNA break and repair involves the recognition (checkpoint) and activation of the repairing system (non-homologous or homologous). From KEGG analysis, we noticed that pathways involved in wound response, tissue remodeling, wound healing, and regulation of apoptosis were significantly affected (Figure 3A). These signaling pathways likely regulate cisplatin-induced testicular injury response and repair/regeneration; therefore, to examine whether nHNK-associated restoration of testicular function involves in the processes mentioned above, we tested the protein

**A**

| GO_accession | Description | p value | Affected Gene Count |
|---|---|---|---|
| GO:0009611 | response to wounding | 1.86E-18 | 136 |
| GO:0048771 | tissue remodeling | 7.42E-18 | 73 |
| GO:0042060 | wound healing | 6.80E-15 | 103 |
| GO:2001233 | regulation of apoptotic signaling pathway | 1.69E-12 | 108 |

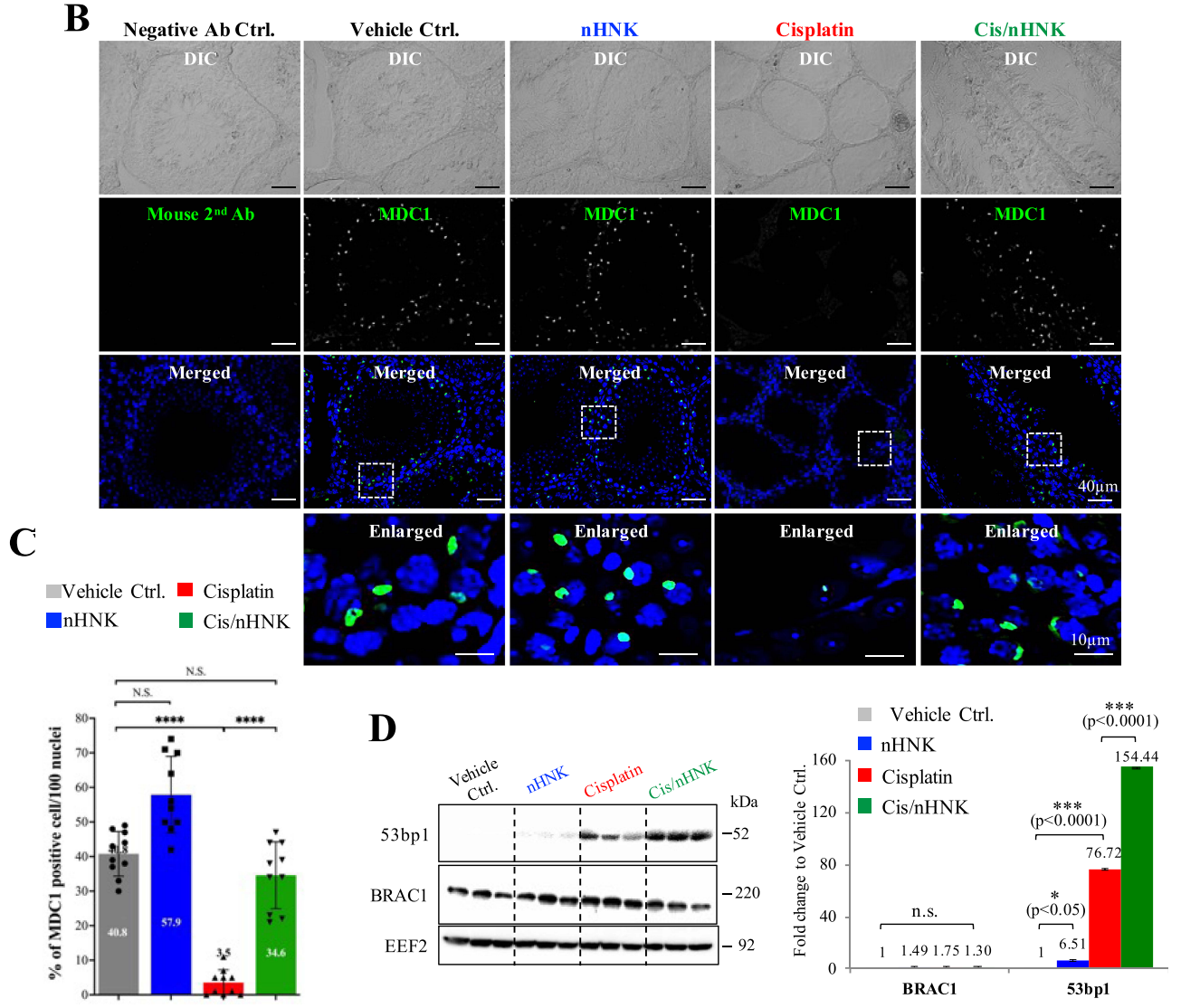


**Figure 3** Antioxidant nanoparticle promoted MDC1-53bp1 associated non-homologous DNA break repair. (**A**) GO analysis showed that in total, 420 genes that were known to involve in the signaling pathways related to wound response, tissue remodeling, wound healing, and apoptosis regulation were highly affected. (**B**) DNA double-strand break checkpoint protein MDC1 was highly expressed in the control nHNK and nHNK treatment groups, indicating that the testicular DNA damage checkpoint and repair mechanism was functional in these groups. In contrast, this mechanism was abolished in the cisplatin group. (**C**) Quantitative data supported the immunofluorescent observation that a significant decrease in the % of MDC1-positive cells (3.5%) was measured in the cisplatin group. And nHNK treatment reversed the protein expression of MDC1 in the testis (34.6%). (**D**) 53bp1-mediated non-homologous DNA repair mechanism was activated upon nHNK treatment, and no changes can be detected regarding the BRAC1-associated homologous DNA repair mechanism. Bars represent standard deviation (S.D.), and results were presented as mean ± standard deviation (S.D.). *p<0.05, ***p<0.001, ****p<0.0001.

**Abbreviation**: N.S., not statistically different.

expression levels of these relevant molecules. As shown in Figure 3B, we observed in control, nHNK alone, and in Cis/nHNK treatment groups, pronounced mediator of DNA damage checkpoint 1 (MDC1) positive signals can be detected in cells located at the outer layer of the seminiferous tubules (Figure 3B and 3C, 40.8%, 57.9%, 34.6% in control, nHNK alone and in Cis/nHNK treatment group, respectively), based on their localization, these positive cells are likely to be the primary spermatocyte. In sharp contrast, cisplatin-injured testis showed significantly less number of MDC1-positive cells (3.5%) (Figure 3B and C). The downstream signaling pathway of MDC1 could be either p53 binding protein 1 (53bp1) or break cancer gene 1 (BRCA1), depending on the cell cycle. Interestingly, we observed no changes in BRCA1 expression between our experimental groups, but a significant increase of 53bp1 expression in the Cis/nHNK group, indicating nHNK provoked 53bp1-associated DNA repair mechanism after cisplatin injury (Figure 3D, supplementary Figure 4).

## Encapsulated Nanoparticles Maintained Mitochondria Integrity and ATP Production

When compared with sperm cells retrieved from control testis, significant adverse effects on sperm swimming patterns, including motility, progressive motility, average path velocity (VAP), velocity straight line (VSL), curvilinear velocity (VCL), and the amplitude of lateral head (ALH) were measured in the cisplatin-injured sperm; in sharp contrast, the parameters mentioned above were significantly restored to the level similar to those of control sperm (Figure 4A). Sperm motility and progressive motility rely on functional mitochondria to produce sufficient ATP as the energy source for the sperm movement.[36] Although we identified down-regulated genes related to the maintenance of the sperm tail or acrosomal structure, we did not observe apparent structural defects regarding the organization of the sperm tail or acrosome (data not shown). Nevertheless, we detected a cluster of mitochondria-associated genes that were down-regulated after cisplatin injury. Many of these genes were responsible for maintaining normal mitochondrial function and structure, such as Misato 1, mitochondrial distribution, morphology regulator, and mitofusin 1, 2 (Figure 4B).

When we examined the structural integrity of the mitochondria and ATP production ability of sperm cells from these groups, in contrast to the well-structured cristate architecture present in the midpiece of control sperm (Figure 4C1), we observed a disrupted and relatively empty mitochondria architecture in both sperm cells and epididymal epithelium

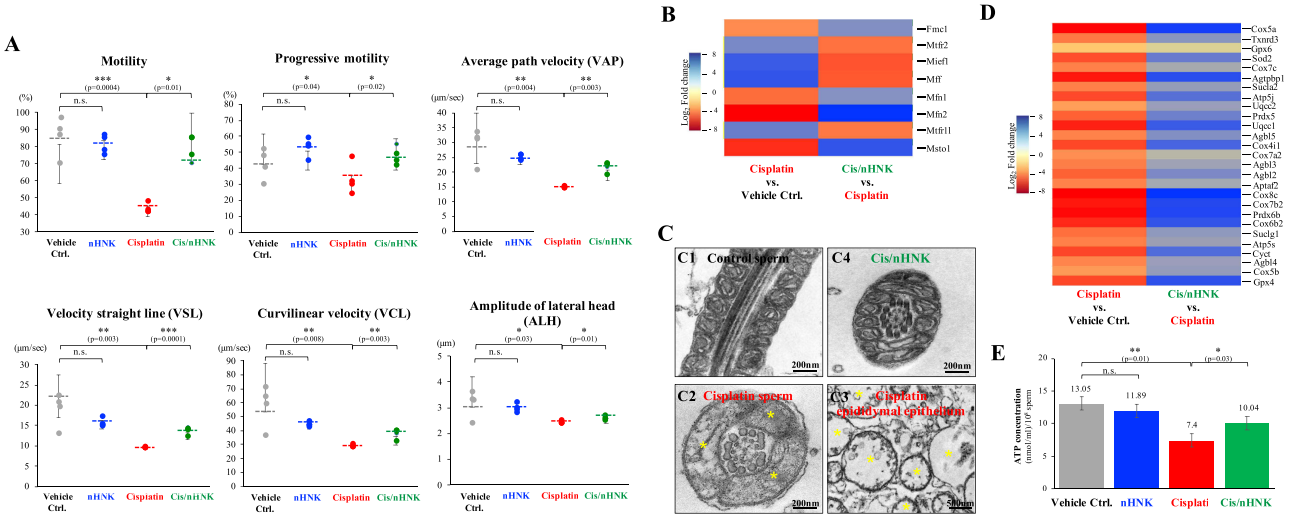


**Figure 4** Sperm motility, mitochondria integrity, and genes associated with mitochondrial antioxidation enzymes were altered upon cisplatin injury and nHNK treatment. (**A**) iSperm analysis on sperm swimming patterns showed a significant decrease in all sperm swimming patterns evaluated, including sperm motility, progressive motility, average path velocity (VAP), velocity straight line (VSL), curvilinear velocity (VCL), the amplitude of lateral head (ALH). These parameters were rescued after nHNK treatment. (**B**) RNAseq analysis showed that several essential genes for mitochondria function and structural integrity, such as Mfn1, 2, and Msto1, were affected. (**C**) In contrast to the well-organized mitochondria cristae structure in the control sperm (C1), cisplatin-injured sperm (C2) and epididymal epithelium (C3) showed disrupted mitochondria structure with the absence of cristae (marked in yellow). The reappearance of mitochondria cristae can be observed under electron microscopy in the sperm cells recovered from the nHNK-treatment testis. (**D**) Genes associated with mitochondrial antioxidant enzymes and ATP synthesis were downregulated upon cisplatin injury. Up-regulation of these gene expressions after nHNK treatment may explain the restored ATP production ability. (**E**) When sperm cells of 4 experimental groups were subjected to ATP assay, a significant decrease in the amount of ATP was measured in the cisplatin injured group, and restoration of ATP synthesis was measured in nHNK sperm. Bars represent standard deviation (S.D.), and results were presented as mean±standard deviation (S.D.). *p<0.05, **p<0.01. Twenty TEM images from each experimental group were evaluated, and representative images were presented.
**Abbreviation**: N.S., not statistically different.

retrieved from the cisplatin-injured mouse (marked in asterisks, Figure 4C2 and C3). And these disrupted mitochondria were partially restored after nHNK treatment (Figure 4C4). The restoration of mitochondrial structure observed after nHNK treatment likely results in the up-regulation of ATP synthesis-related genes and those of antioxidant enzymes (Figure 4D) and may explain the fact that a significantly higher amount of ATP was measured in sperm cells retrieved from Cis/nHNK mice when compared with sperm cells of cisplatin-injured animals (Figure 4E, 13.05, 11.89, 7.4, and 10.04 nmol/mL/$10^8$ sperm for control, nHNK, cisplatin, Cis/nHNK, respectively).

## Honokiol Antioxidant Nanoparticles Promoted Calcium Influx in Sperm

Progressive motility is characterized by the vigorous movement of the sperm tail and is an indication of sperm capacitation upon extracellular calcium influx. We observed significant restoration of both motility and progressive motility in nHNK-treated sperm (Figure 4A). NGS data also showed that numerous calcium-associated genes, such as sperm-specific cation channel (Catsper 1–4), voltage-dependent calcium channel (Cacna1, Cacna1b1), and calcium/calmodulin-dependent protein kinase (Camk2, Camk4) were down-regulated upon cisplatin injury, but were up-regulated after nHNK treatment (Figure 5A). To evaluate whether nHNK actually affects extracellular calcium influx in sperm, we performed a kinetic intracellular calcium measurement using Fluo-4 AM as an indicator in live sperm.[37] Baseline values

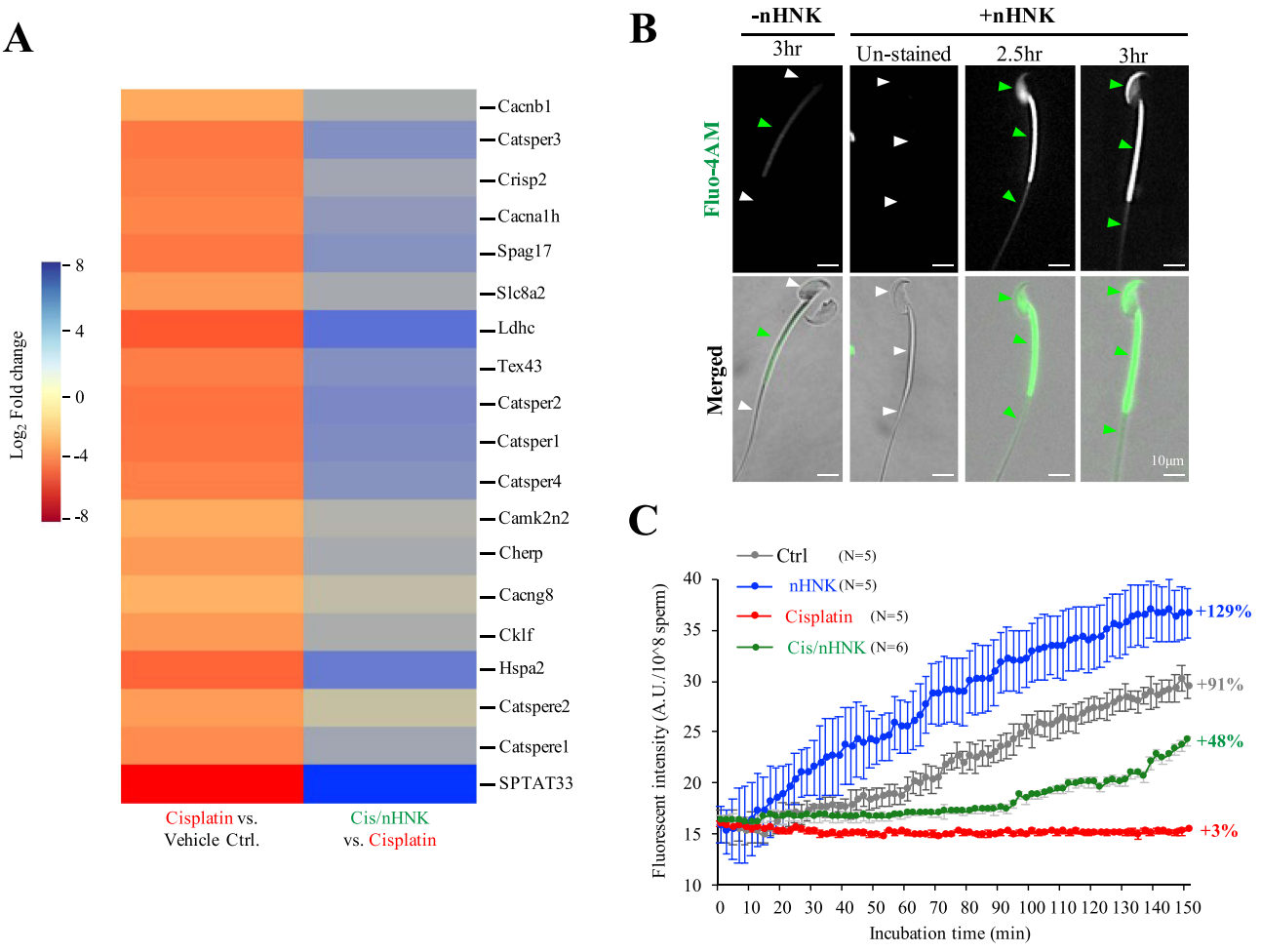


**Figure 5** nHNK promoted sperm calcium influx. (**A**) Genes responsible for calcium regulation were affected. Gene such as Cherp was known to maintain calcium homeostasis and was downregulated upon cisplatin injury. Other genes such as Catspere, CatSper were known to regulate calcium influx in sperm tail and were responsible for sperm motility, were found to be downregulated upon cisplatin injury but were upregulated after nHNK treatment (**B**) To monitor the dynamic calcium influx in sperm cells, live-cell dye, Fluo-4 AM, was used. In contrast to the faint calcium signal observed at the sperm midpiece of non-nHNK incubated sperm, sperm cells co-incubated with nHNK showed strong signals at both sperm head, midpiece, and tail (marked with green arrowheads). (**C**) Dynamic calcium influx was quantitatively assessed. In contrast to the relatively flat pattern measured from sperm cells of cisplatin-injured mice (red line, 3% increase), significant time-dependent increases in calcium flux were measured in sperm cells retrieved from control, nHNK, and nHNK/Cis mice (91%, 129%, and 48% increase in control, nHNK alone, and Cis/nHNK group, respectively).

and background signals were first established and used for later raw value subtraction (Supplementary Figure 2). In contrast to steady background signals throughout the entire measurement period in medium controls (Supplementary Figure 2, blue, grey, black, yellow, and purple lines), a time-dependent increase of $[Ca^{2+}]i$ signal was measured in sperm cells under capacitation conditions (Supplementary Figure 2, orange line). As shown in Figure 5B, when compared to a weak signal detected at the sperm midpiece in sperm cells without nHNK co-incubation (Figure 5B, marked with a green arrowhead), no other signals were detected. In sharp contrast, an intense signal was seen at the midpiece and tail of the sperm cells co-incubated with nHNK for 2.5 hr (Figure 5B, marked with green arrowheads). And after prolonged nHNK co-incubation of 3 hr, an additional signal can be detected at the acrosome region (Figure 5B, marked with green arrowheads). We also showed that when compared with defected calcium influx in cisplatin-injury sperm (+3% when compared with its own time 0, red line in Figure 5C), nHNK treatment of cisplatin-injured sperm profoundly restored the ability of intracellular calcium influx (+48% when compared with its own time 0, green line in Figure 5C) after 2.5 hr incubation in the capacitation medium (Figure 5C). Together with the profound detection of intracellular calcium in nHNK alone group (+129% when compared with its own time 0, Figure 5C, blue line), we demonstrated that honokiol nanoparticles restored and promoted calcium influx in sperm.

## Discussion

When treating cancer patients, chemotherapy is one of the major therapeutic options; however, upon eradicating cancer cells, the accompanied off-target damages to normal tissue are inevitable. The mechanism of cisplatin-induced cytotoxicity and organ failure is not only due to cell cycle arrest or DNA damages;[38–43] oxidative and nitrosative stresses induced by cisplatin have also been reported.[13,39,42,44–47] Earlier studies, including ours, showed that cisplatin bound not only to the nuclear DNA but also to the mitochondria DNA (mtDNA).[13,44,45,47] The formation of DNA adducts arrested the cell cycle and disrupted the mitochondria electron transport chain and mitochondrial antioxidant enzyme synthesis/activity. These alterations mentioned above resulted in ROS overproduction and compromised endogenous antioxidation defense mechanisms that led to cytotoxic effects in both cancer and normal cells.[40,43,48] Our earlier study demonstrated that platinum-based chemotherapy caused severe renal and testicular damage and fibrosis due to impaired mitochondria function, increased endoplasmic reticulum stress, cellular apoptosis, disrupted renal epithelium, and seminiferous tubule structure.[14,15] The evidence mentioned above demonstrates that cisplatin-based chemotherapy results in severe accumulation of free radicals, resulting in oxidative stress and functional disturbance of vital organs, such as kidneys and testis.

One of the many known biological functions of the natural polyphenol compound honokiol is to act as a free radical scavenger to reduce the accumulation of excessive ROS. However, earlier studies showed that HNK is a lipophilic polyphenol compound that exhibited poor tissue distribution and solubility when given directly; by encapsulating HNK into liposome-based nanoparticles, cellular availability, targeted tissue or cellular distribution can be optimized.[49–52] Our RNAseq analysis indicated that besides the known roles in regulating oxidative stress responses, genes related to spermatogenesis and sperm motility were also altered upon nHNK administration. We observed that upon nHNK treatment, a cell proliferation marker Ki67 and spermatogenesis marker KIF11 protein expression levels were upregulated and presented at the seminiferous tubules' outer layer where spermatogonium and primary spermatocyte locate, suggesting nHNK treatment promotes testicular cell proliferation and the subsequent restoration of spermatogenesis. These positive effects are in agreement with our earlier study showing an increase in sperm concentration and the restoration of the testicular structure,[15] and are likely account for the reappearance of multi-spermatogenic layers observed in the testis. Another interesting finding was that nHNK treatment promoted testicular double-strand DNA break checkpoint protein MDC1 expression and the activation of the downstream 53bp1 DNA repair mechanism.[53,54] Activation of this non-homologous DNA repair mechanism could mitigate the negative outcome of cisplatin-induced DNA damage. Together with enhanced cell proliferation and spermatogenesis, normal testis function could therefore be restored.

Of particular interest is that compared to the immotile or weakly tail-beating sperm cells recovered from cisplatin-injured mice, the restoration of sperm motility after nHNK treatment is likely associated with improved sperm mitochondria integrity and the subsequent ATP-producing function as an apparent recovery of mitochondria cristae structure and ATP production were noted. Maintaining sperm motility needs functional mitochondria to produce

sufficient ATP as the energy source and intracellular calcium oscillation and calcium influx through various cation or calcium channels located at the sperm midpiece and tail.[55–57] The most significant sperm ion channel is the cation channel of sperm (CatSper), a sperm-specific $Ca^{2+}$ channel required for the hyperactivation of the sperm motility.[4,56] Other ion channels, such as voltage-gated $Ca^{2+}$ channels (VGCCs), $Ca^{2+}$-activated Cl-channels (CaCCs), and SLO $K^{+}$ channels are to ensure the activation and modulation of CatSper.[57] We showed that cisplatin downregulated many calcium channel-related genes, including CatSper 1, 2, 4; using Fluo-4 AM, a live cell calcium dye, we detected that cisplatin disrupted intracellular sperm calcium influx, but the application of nHNK could recover ~50% of the regular calcium influx to the sperm cells; however, how honokiol affects calcium channel require further studies. However, an ATP-driven calcium channel is likely involved. A recent paper from Miyata et al also demonstrated that SPATA33 interacts with sperm calcineurin, a calcium-dependent phosphatase, and localizes calcineurin to the mitochondria and regulates sperm motility.[58] We noted that testicular SPATA33 gene expression was significantly downregulated upon cisplatin injury and was upregulated after nHNK administration; moreover, we also saw that upon our in vitro incubation of sperm cells with nHNK, besides the observed calcium influx at the sperm tail, a pronounced increase in calcium influx was also detected at the sperm midpiece; thus, the increased total calcium influx detected is likely contributed from increase calcium influx in both sperm midpiece and tail which is beneficial for the restoration of sperm motility.

## Conclusions

In conclusion, based on evidence provided in the current study, natural polyphenol extracts honokiol acts not only as a ROS scavenger that reduces the intracellular accumulation of ROS but it also protects the mitochondrial structure and maintains the ATP-producing ability of testicular and sperm cells. By a yet-to-be-elucidated promotion of intracellular calcium influx, sperm motility is restored. Moreover, by activating a non-homologous DNA repair mechanism, honokiol mitigates cisplatin-induced DNA double-strand break and promotes spermatogenesis. A schematic illustration is summarized in Figure 6. Taken together, the nanoparticulated antioxidant might benefit patients undertaking cisplatin-based chemotherapy and could restore their sperm quality and fertilization ability.

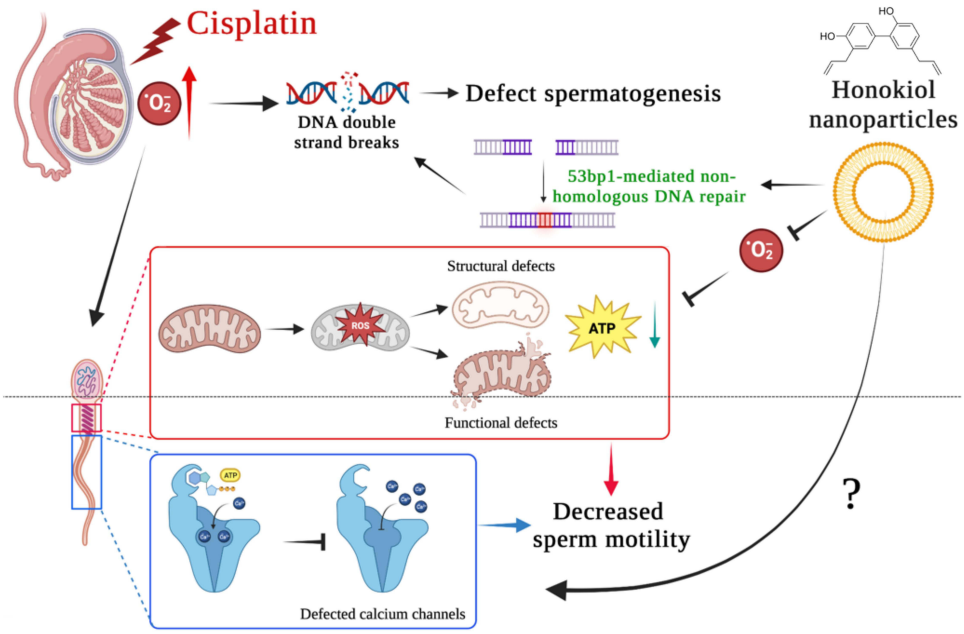


**Figure 6** Summarized findings of the current study. Cisplatin results in the overproduction of free radicals and leads to oxidative stress and damage in the testis. Accumulation of excessive free radicals leads to DNA double-strand breaks that disrupt normal spermatogenesis. Cisplatin-induced oxidative stress also causes structural and functional defects of sperm mitochondria, which further compromise normal ATP production. In combination with insufficient ATP and defected calcium channel, the calcium influx required for sperm hypermotility was likely affected as sperm progressive motility was decreased significantly, and sperm motility was affected. Natural polyphenol extracts honokiol encapsulated within nanoparticles serve as a ROS scavenger that overcomes mitochondrial oxidative damage and promotes 53bp1-associated non-homologous DNA repair mechanism. With a yet-uncovered mechanism promoting sperm calcium influx, nHNK treatment mitigates cisplatin-induced male fertility defects.

## Data Sharing Statement

Original raw data presented in this study are available upon reasonable request.

## Ethics Approval and Information Consent

Ethics approval (NTU109-EL-00158), including all aspects of animal experiments, tissue sample collection, and animal carcass handling, were performed and supervised by the approved veterinarians throughout routine veterinary health management under the permission of institutional animal care and use committee (IACUC) protocols at National Taiwan University. Patient consent statement is not applicable.

## Consent for Publication

We confirm that the details of any images, videos, recordings, etc can be published and that all authors have shown the article contents to be published.

## Acknowledgments

We thank NTU Mass Spectrometry Platform, Electron Microscopy Core Facility (College of Bioresources and Agriculture) for the technical support. The preparation of liposome-based nanoparticles by Prof. Hong-Jen Liang from the Department of Food Science, Yuanpei University, Taiwan, is also acknowledged.

## Author Contributions

All authors made a significant contribution to the work reported. YSW, YLC, WYL, YYY, TEW, PST contributed to the execution of all experimental work and data acquisition; YSW, WYL, SJL, CHW, JIY, PST contributed to the initial study designed; YLC, TEW, WYL, YYY, JSY, PST performed data analyses and data interpretation; YSW, JSY, PST contributed to data organization, drafted and revised the manuscript. All authors gave final approval of the version to be published, have agreed on the journal to which the article has been submitted, and agreed to be accountable for all aspects of the work.

## Funding

This study was financially supported by the National Science Council, Taiwan (grant# 109-2313-B-002-002-MY2) and by the Ministry of Education, Taiwan (grant# NTU-CC-110L893002, NTU-CC-111L892402, NTU-CC-112L891302 to PSJ TSAI).

## Disclosure

All authors declare no conflict of interest that could prejudice the impartiality of the research reported.

## References

1. Clark GF. Molecular models for mouse sperm-oocyte binding. *Glycobiology*. 2011;21(1):3–5. doi:10.1093/glycob/cwq159
2. Tosti E, Menezo Y. Gamete activation: basic knowledge and clinical applications. *Hum Reprod Update*. 2016;22(4):420–439. doi:10.1093/humupd/dmw014
3. Finkelstein M, Etkovitz N, Breitbart H. Ca(2+) signaling in mammalian spermatozoa. *Mol Cell Endocrinol*. 2020;516:110953. doi:10.1016/j.mce.2020.110953
4. Wang H, McGoldrick LL, Chung JJ. Sperm ion channels and transporters in male fertility and infertility. *Nat Rev Urol*. 2021;18(1):46–66. doi:10.1038/s41585-020-00390-9
5. Lishko PV, Kirichok Y, Ren D, et al. The control of male fertility by spermatozoan ion channels. *Annu Rev Physiol*. 2012;74(1):453–475. doi:10.1146/annurev-physiol-020911-153258
6. Ren D, Navarro B, Perez G, et al. A sperm ion channel required for sperm motility and male fertility. *Nature*. 2001;413(6856):603–609. doi:10.1038/35098027
7. Lefievre L, Nash K, Mansell S, et al. 2-APB-potentiated channels amplify CatSper-induced Ca(2+) signals in human sperm. *Biochem J*. 2012;448(2):189–200. doi:10.1042/BJ20120339
8. Hirohashi N, Yanagimachi R. Sperm acrosome reaction: its site and role in fertilization. *Biol Reprod*. 2018;99(1):127–133. doi:10.1093/biolre/ioy045
9. Tsai PS, Garcia-Gil N, van Haeften T, et al. How pig sperm prepares to fertilize: stable acrosome docking to the plasma membrane. *PLoS One*. 2010;5(6):e11204. doi:10.1371/journal.pone.0011204
10. Boguenet M, Bouet P-E, Spiers A, et al. Mitochondria: their role in spermatozoa and in male infertility. *Hum Reprod Update*. 2021;27(4):697–719. doi:10.1093/humupd/dmab001

11. Losano JDA, Angrimani DDSR, Ferreira Leite R, et al. Spermatic mitochondria: role in oxidative homeostasis, sperm function and possible tools for their assessment. *Zygote*. 2018;26(4):251–260. doi:10.1017/S0967199418000242
12. Vertika S, Singh KK, Rajender S. Mitochondria, spermatogenesis, and male infertility - An update. *Mitochondrion*. 2020;54:26–40. doi:10.1016/j.mito.2020.06.003
13. Choi Y-M, Kim H-K, Shim W, et al. Mechanism of cisplatin-induced cytotoxicity is correlated to impaired metabolism due to mitochondrial ROS generation. *PLoS One*. 2015;10(8):e0135083. doi:10.1371/journal.pone.0135083
14. Liu HT, Wang T-E, Hsu Y-T, et al. Nanoparticulated honokiol mitigates cisplatin-induced chronic kidney injury by maintaining mitochondria antioxidant capacity and reducing caspase 3-associated cellular apoptosis. *Antioxidants*. 2019;8(10):466. doi:10.3390/antiox8100466
15. Wang TE, Lai Y-H, Yang K-C, et al. Counteracting cisplatin-induced testicular damages by natural polyphenol constituent honokiol. *Antioxidants*. 2020;9(8):723. doi:10.3390/antiox9080723
16. Sharma P, Sampath H. Mitochondrial DNA integrity: role in health and disease. *Cells*. 2019;8(2):100. doi:10.3390/cells8020100
17. Chainy GBN, Sahoo DK. Hormones and oxidative stress: an overview. *Free Radic Res*. 2020;54(1):1–26. doi:10.1080/10715762.2019.1702656
18. Poprac P, Jomova K, Simunkova M, et al. Targeting free radicals in oxidative stress-related human diseases. *Trends Pharmacol Sci*. 2017;38(7):592–607. doi:10.1016/j.tips.2017.04.005
19. Aitken RJ. Impact of oxidative stress on male and female germ cells: implications for fertility. *Reproduction*. 2020;159(4):R189–R201. doi:10.1530/REP-19-0452
20. Alahmar AT. Role of oxidative stress in male infertility: an updated review. *J Hum Reprod Sci*. 2019;12(1):4–18. doi:10.4103/jhrs.JHRS_150_18
21. Bansal AK, Bilaspuri GS. Impacts of oxidative stress and antioxidants on semen functions. *Vet Med Int*. 2010;2010. doi:10.4061/2011/686137
22. Takeshima T, Usui K, Mori K, et al. Oxidative stress and male infertility. *Reprod Med Biol*. 2021;20(1):41–52. doi:10.1002/rmb2.12353
23. Gupta S, Finelli R, Agarwal A, et al. Total antioxidant capacity-Relevance, methods and clinical implications. *Andrologia*. 2021;53(2):e13624. doi:10.1111/and.13624
24. Miyamoto Y, Koh YH, Park YS, et al. Oxidative stress caused by inactivation of glutathione peroxidase and adaptive responses. *Biol Chem*. 2003;384(4):567–574. doi:10.1515/BC.2003.064
25. Mruk DD, Silvestrini B, Mo M-Y, et al. Antioxidant superoxide dismutase - a review: its function, regulation in the testis, and role in male fertility. *Contraception*. 2002;65(4):305–311. doi:10.1016/S0010-7824(01)00320-1
26. O'Flaherty C. Orchestrating the antioxidant defenses in the epididymis. *Andrology*. 2019;7(5):662–668. doi:10.1111/andr.12630
27. O'Flaherty C, Boisvert A, Manku G, et al. Protective role of peroxiredoxins against reactive oxygen species in neonatal rat testicular gonocytes. *Antioxidants*. 2019;9(1):32. doi:10.3390/antiox9010032
28. Rahman SU, Huang Y, Zhu L, et al. Therapeutic role of green tea polyphenols in improving fertility: a review. *Nutrients*. 2018;10(7):834. doi:10.3390/nu10070834
29. Shaito A, Posadino AM, Younes N, et al. Potential adverse effects of resveratrol: a literature review. *Int J Mol Sci*. 2020;21(6):2084. doi:10.3390/ijms21062084
30. Wang TJ, Liu H-T, Lai Y-H, et al. Honokiol, a polyphenol natural compound, attenuates cisplatin-induced acute cytotoxicity in renal epithelial cells through cellular oxidative stress and cytoskeleton modulations. *Front Pharmacol*. 2018;9:357. doi:10.3389/fphar.2018.00357
31. Ijaz MU, Tahir A, Ahmed H, et al. Chemoprotective effect of vitexin against cisplatin-induced biochemical, spermatological, steroidogenic, hormonal, apoptotic and histopathological damages in the testes of Sprague-Dawley rats. *Saudi Pharm J*. 2022;30(5):519–526. doi:10.1016/j.jsps.2022.03.001
32. Hsiao YP, Chen H-T, Liang Y-C, et al. Development of nanosome-encapsulated honokiol for intravenous therapy against experimental autoimmune encephalomyelitis. *Int J Nanomedicine*. 2020;15:17–29. doi:10.2147/IJN.S214349
33. Wang TE, Li S-H, Minabe S, et al. Mouse quiescin sulfhydryl oxidases exhibit distinct epididymal luminal distribution with segment-specific sperm surface associations. *Biol Reprod*. 2018;99(5):1022–1033. doi:10.1093/biolre/ioy125
34. Wang TE, Minabe S, Matsuda F, et al. Testosterone regulation on quiescin sulfhydryl oxidase 2 synthesis in the epididymis. *Reproduction*. 2021;161(5):593–602. doi:10.1530/REP-20-0629
35. Hara-Yokoyama M, Kurihara H, Ichinose S, et al. KIF11 as a potential marker of spermatogenesis within mouse seminiferous tubule cross-sections. *J Histochem Cytochem*. 2019;67(11):813–824. doi:10.1369/0022155419871027
36. Balbach M, Beckert V, Hansen JN, et al. Shedding light on the role of cAMP in mammalian sperm physiology. *Mol Cell Endocrinol*. 2018;468:111–120. doi:10.1016/j.mce.2017.11.008
37. Sampaio B, Ortiz I, Resende H, et al. Factors affecting intracellular calcium influx in response to calcium ionophore A23187 in equine sperm. *Andrology*. 2021;9(5):1631–1651. doi:10.1111/andr.13036
38. Ciarimboli G, Deuster D, Knief A, et al. Organic cation transporter 2 mediates cisplatin-induced oto- and nephrotoxicity and is a target for protective interventions. *Am J Pathol*. 2010;176(3):1169–1180. doi:10.2353/ajpath.2010.090610
39. Dasari S, Tchounwou PB. Cisplatin in cancer therapy: molecular mechanisms of action. *Eur J Pharmacol*. 2014;740:364–378. doi:10.1016/j.ejphar.2014.07.025
40. Zhu S, Pabla N, Tang C, et al. DNA damage response in cisplatin-induced nephrotoxicity. *Arch Toxicol*. 2015;89(12):2197–2205. doi:10.1007/s00204-015-1633-3
41. Dugbartey GJ, Peppone LJ, de Graaf IAM. An integrative view of cisplatin-induced renal and cardiac toxicities: molecular mechanisms, current treatment challenges and potential protective measures. *Toxicology*. 2016;371:58–66. doi:10.1016/j.tox.2016.10.001
42. Ozkok A, Edelstein CL. Pathophysiology of cisplatin-induced acute kidney injury. *Biomed Res Int*. 2014;2014:967826. doi:10.1155/2014/967826
43. Garcia Sar D, Montes-Bayón M, Blanco González E, et al. Speciation studies of cisplatin adducts with DNA nucleotides via elemental specific detection (P and Pt) using liquid chromatography-inductively coupled plasma-mass spectrometry and structural characterization by electrospray mass spectrometry. *J Anal At Spectrom*. 2006;21(9):861–868. doi:10.1039/B603434A
44. Cullen KJ, Yang Z, Schumaker L, et al. Mitochondria as a critical target of the chemotherapeutic agent cisplatin in head and neck cancer. *J Bioenerg Biomembr*. 2007;39(1):43–50. doi:10.1007/s10863-006-9059-5
45. Marullo R, Werner E, Degtyareva N, et al. Cisplatin induces a mitochondrial-ROS response that contributes to cytotoxicity depending on mitochondrial redox status and bioenergetic functions. *PLoS One*. 2013;8(11):e81162. doi:10.1371/journal.pone.0081162

46. Santos NA, Bezerra CSC, Martins NM, et al. Hydroxyl radical scavenger ameliorates cisplatin-induced nephrotoxicity by preventing oxidative stress, redox state unbalance, impairment of energetic metabolism and apoptosis in rat kidney mitochondria. *Cancer Chemother Pharmacol*. 2008;61(1):145–155. doi:10.1007/s00280-007-0459-y
47. Wang FY, Tang X-M, Wang X, et al. Mitochondria-targeted platinum(II) complexes induce apoptosis-dependent autophagic cell death mediated by ER-stress in A549 cancer cells. *Eur J Med Chem*. 2018;155:639–650. doi:10.1016/j.ejmech.2018.06.018
48. Miller RP, Tadagavadi RK, Ramesh G, et al. Mechanisms of cisplatin nephrotoxicity. *Toxins*. 2010;2(11):2490–2518. doi:10.3390/toxins2112490
49. Zhang X, Chen H, Zhang Y, et al. HA-DOPE-modified honokiol-loaded liposomes targeted therapy for osteosarcoma. *Int J Nanomedicine*. 2022;17:5137–5151. doi:10.2147/IJN.S371934
50. Zhang Q, Li D, Guan S, et al. Tumor-targeted delivery of honokiol via polysialic acid modified zein nanoparticles prevents breast cancer progression and metastasis. *Int J Biol Macromol*. 2022;203:280–291. doi:10.1016/j.ijbiomac.2022.01.148
51. Weng Y, Zhang H, Xu S, et al. Preparation and quality evaluation of honokiol nanoparticles using a new polysaccharide polymer as its carrier. *Curr Drug Deliv*. 2023;20(2):183–191. doi:10.2174/1567201819666220607153457
52. Li X, Guan S, Li H, et al. Polysialic acid-functionalized liposomes for efficient honokiol delivery to inhibit breast cancer growth and metastasis. *Drug Deliv*. 2023;30(1):2181746. doi:10.1080/10717544.2023.2181746
53. Huang RX, Zhou PK. DNA damage response signaling pathways and targets for radiotherapy sensitization in cancer. *Signal Transduct Target Therc*. 2020;5(1):60.
54. Noordermeer SM, Adam S, Setiaputra D, et al. The shieldin complex mediates 53BP1-dependent DNA repair. *Nature*. 2018;560(7716):117–121. doi:10.1038/s41586-018-0340-7
55. Mata-Martinez E, Sánchez-Cárdenas C, Chávez JC, et al. Role of calcium oscillations in sperm physiology. *Biosystems*. 2021;209:104524. doi:10.1016/j.biosystems.2021.104524
56. Lishko PV, Mannowetz N. CatSper: a unique calcium channel of the sperm flagellum. *Curr Opin Physiol*. 2018;2:109–113. doi:10.1016/j.cophys.2018.02.004
57. Nowicka-Bauer K, Szymczak-Cendlak M. Structure and function of ion channels regulating sperm motility-an overview. *Int J Mol Sci*. 2021;22(6):3259. doi:10.3390/ijms22063259
58. Miyata H, Satouh Y, Mashiko D, et al. Sperm calcineurin inhibition prevents mouse fertility with implications for male contraceptive. *Science*. 2015;350(6259):442–445. doi:10.1126/science.aad0836